Article

Influence of the Environment on the [4Fe–4S] to [2Fe–2S] Cluster Switch in the Transcriptional Regulator FNR

Jason C. Crack, Alisa A. Gaskell, Jeffrey Green, Myles R. Cheesman, Nick E. Le Brun, and Andrew J. Thomson

J. Am. Chem. Soc., **2008**, 130 (5), 1749-1758 • DOI: 10.1021/ja077455+

J|A|C|S
ARTICLES
Published on Web 01/11/2008

Influence of the Environment on the $[4Fe-4S]^{2+}$ to $[2Fe-2S]^{2+}$ Cluster Switch in the Transcriptional Regulator FNR

Jason C. Crack,[†] Alisa A. Gaskell,[†] Jeffrey Green,[‡] Myles R. Cheesman,[†] Nick E. Le Brun,*[,†] and Andrew J. Thomson*[,†]

Centre for Metalloprotein Spectroscopy and Biology, School of Chemical Sciences and Pharmacy, University of East Anglia, Norwich, NR4 7TJ, U.K., and the Department of Molecular Biology and Biotechnology, University of Sheffield, Sheffield S10 2TN, U.K.

Received September 27, 2007; E-mail: A.Thomson@uea.ac.uk; n.le-brun@uea.ac.uk

Abstract: In *Escherichia coli*, the switch between aerobic and anaerobic metabolism is primarily controlled by the fumarate and nitrate reduction transcriptional regulator FNR. In the absence of O_2, FNR binds a $[4Fe-4S]^{2+}$ cluster, generating a transcriptionally active dimeric form. Exposure to O_2 results in the conversion of the cluster to a $[2Fe-2S]^{2+}$ form, leading to dissociation of the protein into transcriptionally inactive monomers. The $[4Fe-4S]^{2+}$ to $[2Fe-2S]^{2+}$ cluster conversion proceeds in two steps. Step 1 involves the one-electron oxidation of the cluster, resulting in the release of Fe^{2+}, generating a $[3Fe-4S]^{1+}$ cluster intermediate, and a superoxide ion. In step 2, the cluster intermediate spontaneously rearranges to form the $[2Fe-2S]^{2+}$ cluster, with the release of a Fe^{3+} ion and two sulfide ions. Here, we demonstrate that, in both native and reconstituted [4Fe−4S] FNR, the reaction environment and, in particular, the presence of Fe^{2+} and/or Fe^{3+} chelators can influence significantly the cluster conversion reaction. We demonstrate that while the rate of step 1 is largely insensitive to chelators, that of step 2 is significantly enhanced by both Fe^{2+} and Fe^{3+} chelators. We show that, for reactions in Fe^{3+}-coordinating phosphate buffer, step 2 is enhanced to the extent that step 1 becomes the rate determining step and the $[3Fe-4S]^{1+}$ intermediate is no longer detectable. Furthermore, Fe^{3+} released during this step is susceptible to reduction in the presence of Fe^{2+} chelators. This work, which may have significance for the *in vivo* FNR cluster conversion reaction in the cell cytoplasm, provides an explanation for apparently contradictory results reported from different laboratories.

Introduction

Bacteria exhibit a remarkable capacity to adapt to their environment, as illustrated by their ability to utilize oxygen as the respiratory terminal electron acceptor and a range of other acceptors when oxygen is scarce. In *Escherichia coli*, an oxygen-sensing transcription regulating protein called FNR orchestrates the switch over between aerobic and anaerobic respiration.[1−3] FNR belongs to a growing family of transcriptional regulators that initiate physiological changes in response to a variety of environmental and metabolic stimuli.[4−6] *E. coli* cAMP receptor protein (CRP) is the archetypal member of this family, and the high-resolution structure of CRP revealed a fold that provides a versatile system for transducing either environmental or metabolic signals into a physiological response.[5−7] Based on sequence homology, FNR, like CRP, consists of two distinct domains that provide DNA-binding and sensory functions;[7,8] see Figure 1. The C-terminal DNA-binding domain recognizes specific FNR-binding sequences within FNR-controlled promoters.[9] The N-terminal sensory domain contains five cysteine residues, four of which (Cys20, 23, 29, and 122) are essential and capable of binding either a $[4Fe-4S]^{2+}$ or a $[2Fe-2S]^{2+}$ cluster.[10−12]

FNR becomes active under anaerobic conditions through the acquisition of one $[4Fe-4S]^{2+}$ cluster per protein,[11−14] which leads to dimerization and enhances site specific DNA-binding to target promoters.[15,16] Molecular oxygen triggers the conversion of the $[4Fe-4S]^{2+}$ cluster into a $[2Fe-2S]^{2+}$ cluster, both *in vivo* and *in vitro*, causing a conformational change within the protein that in turn leads the protein to dissociate into

[†]University of East Anglia.
[‡]University of Sheffield.

(1) Green, J.; Paget, M. S. *Nat. Rev. Microbiol.* **2004**, *2*, 954−966.
(2) Guest, J. R. *Phil. Trans. R. Soc. London, Ser. B* **1995**, *350*, 189−202.
(3) Guest, J. R. *J. Gen. Microbiol.* **1992**, *138*, 2253−2263.
(4) Green, J.; Scott, C.; Guest, J. R. *Adv. Microb. Physiol.* **2001**, *44*, 1−34.
(5) Korner, H.; Sofia, H. J.; Zumft, W. G. *FEMS Microbiol. Rev.* **2003**, *27*, 559−592.
(6) Spiro, S. *Antonie Van Leeuwenhoek* **1994**, *66*, 23−36.
(7) Schultz, S. C.; Shields, G. C.; Steitz, T. A. *Science* **1991**, *253*, 1001−1007.
(8) Shaw, D. J.; Rice, D. W.; Guest, J. R. *J. Mol. Biol.* **1983**, *166*, 241−247.
(9) Spiro, S.; Gaston, K. L.; Bell, A. I.; Roberts, R. E.; Busby, S. J.; Guest, J. R. *Mol. Microbiol.* **1990**, *4*, 1831−1838.
(10) Green, J.; Sharrocks, A. D.; Green, B.; Geisow, M.; Guest, J. R. *Mol. Microbiol.* **1993**, *8*, 61−68.
(11) Khoroshilova, N.; Popescu, C.; Munck, E.; Beinert, H.; Kiley, P. J. *Proc. Natl. Acad. Sci. U.S.A.* **1997**, *94*, 6087−6092.
(12) Kiley, P. J.; Beinert, H. *FEMS Microbiol. Rev.* **1999**, *22*, 341−352.
(13) Green, J.; Bennett, B.; Jordan, P.; Ralph, E. T.; Thomson, A. J.; Guest, J. R. *Biochem. J.* **1996**, *316*, 887−892.
(14) Crack, J.; Green, J.; Thomson, A. J. *J. Biol. Chem.* **2004**, *279*, 9278−9286.
(15) Khoroshilova, N.; Beinert, H.; Kiley, P. J. *Proc. Natl. Acad. Sci. U.S.A.* **1995**, *92*, 2499−2503.
(16) Lazazzera, B. A.; Bates, D. M.; Kiley, P. J. *Genes Dev.* **1993**, *7*, 1993−2005.

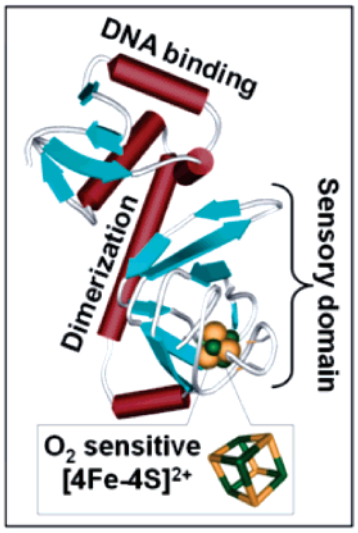

Figure 1. Predicted structure of an FNR monomer. The proposed structure of an FNR monomer, based upon homology with CRP. The location of the [4Fe−4S] binding sensory domain, the dimerization helix, the DNA binding domain, and DNA recognition helix are shown. The model was generated using Swiss-Model and the Swiss-PDB viewer[39] using the CRP X-ray structure as a template.[7]

monomers, thereby abolishing high affinity sequence-specific DNA binding and favorable interactions with the transcription machinery.[11,13−15,17−19]

The mechanism of the oxygen-mediated $[4Fe-4S]^{2+}$ to $[2Fe-2S]^{2+}$ conversion is of considerable current interest. Recently, using a novel assay employing Ellman's reagent, we reported the detection of ∼2 sulfide ions released per FNR monomer during cluster conversion,[20] demonstrating that cluster oxidation is metal based and ruling out alternative mechanistic schemes proposed by others in which sulfide is oxidized to S^0.[21] An essentially complete description of the FNR cluster conversion reaction was very recently achieved, showing that the reaction proceeds in two steps. Step 1 entails the second-order reaction between [4Fe−4S] FNR and oxygen, involving a one electron redox reaction that results in a $[3Fe-4S]^{1+}$ cluster, and the release of one superoxide and Fe^{2+} ion;[22] see eq 1.

Step 1:

$$[4Fe-4S]^{2+} + O_2 \rightarrow [3Fe-4S]^{1+} + Fe^{2+} + O_2^{-\bullet} \quad (1)$$

Step 2 involves the spontaneous (first order) decay of the $[3Fe-4S]^{1+}$, generating the $[2Fe-2S]^{2+}$ cluster, with the release of a Fe^{3+} ion and two sulfide ions;[20] see eq 2.

Step 2:

$$[3Fe-4S]^{1+} \rightarrow [2Fe-2S]^{2+} + Fe^{3+} + 2S^{2-} \quad (2)$$

The overall reaction can be written as in eq 3.

Overall:

$$[4Fe-4S]^{2+} + O_2 \rightarrow [2Fe-2S]^{2+} + Fe^{2+} + Fe^{3+} + 2S^{2-} + O_2^{-\bullet} \quad (3)$$

These data, at first inspection, do not appear to be consistent with previous reports of the FNR oxygen reaction, in which it was reported that ∼2 Fe^{2+} ions are released from the $[4Fe-4S]^{2+}$ cluster during oxygen-induced conversion.[21] Our attention was drawn to differences in the solution environment in which the reaction was taking place and, in particular, to the presence or absence of Fe^{2+} and/or Fe^{3+} chelators that could influence the overall reaction.

To explore how the conversion reaction is influenced by its environment, we have investigated the effect of chelators on the [4Fe−4S] FNR oxygen reaction. Here, using UV−visible absorbance and EPR spectroscopic studies of both native and reconstituted FNR we demonstrate that step 1 is largely unaffected by the presence of either Fe^{2+} or Fe^{3+} chelators. In contrast, step 2 is sensitive to both chelator types, to such an extent that step 1 and step 2 can become kinetically indistinguishable. In addition, in the presence of Fe^{2+} chelators, the Fe^{3+} ion released during step 2 is susceptible to reduction. This is tempered by the presence of an Fe^{3+} chelator. The *in vivo* relevance of the influence of the environment on the FNR reaction is discussed.

Experimental Section

Purification of Native [4Fe−4S] FNR. Native FNR protein was overproduced in aerobic cultures of JRG5369 (*E. coli* BL21λDE3 pGS1859)[20] in an M9 medium[23] supplemented with 0.2% (w/v) glucose, 0.2% (w/v) casamino acids, 1 mM $MgCl_2$, 2 μg/mL thiamine, 20 μM ferric ammonium citrate, and 100 mg/L ampicillin. FNR overproduction was initiated by the addition of isopropyl β-D-thiogalactopyranoside (IPTG, 0.4 mM) (1 h, 37 °C) when $A_{600\ nm}$ reached ∼0.5. To promote formation of [4Fe−4S] FNR *in vivo*, cultures were subsequently sparged with oxygen-free nitrogen gas at 4 °C overnight, essentially as described by Sutton and co-workers,[24] except that cultures were first chilled on ice for 5 to 10 min and supplemented with 200 μM ferric ammonium citrate, 50 μM L-methionine, and 0.001% (*v*/*v*) antifoam 204 (Sigma) prior to sparging. Cells were harvested by transferring anaerobic cultures to O-ring sealed centrifuge tubes (Beckman) and centrifuging at 6500 × *g* for 10 min at 4 °C. Unless otherwise stated, all subsequent work and manipulations were performed under strictly anaerobic conditions in an anaerobic cabinet (Belle Technology), typically operating at ≤2.0 ppm O_2 by volume. All buffers were sparged with oxygen-free nitrogen gas for a minimum of 2 h before introduction into the anaerobic cabinet. Plastic items were equilibrated in an anaerobic cabinet for a minimum of 24 h prior to use. The anaerobic cabinet was also equipped with a specially designed fridge−freezer for anaerobic sample storage (Belle Technology) and fitted with a liquid nitrogen access port.

Cell pellets were resuspended in CelLytic lysis buffer (CelLytic B 10× (Sigma)) diluted 10-fold with buffer A (10 mM potassium phosphate, 100 mM KCl, 10% (v/v) glycerol, pH 6.8) and lysozyme (21.3 μg/mL), DNase I (0.5 μg/mL), 0.1 mM phenylmethanesulphonyl fluoride, and 1 mM benzamidine added. The suspension was thoroughly mixed and incubated at ambient temperature for 15 min. The cell lysate was transferred to O-ring sealed centrifuge tubes (Nalgene) and centrifuged outside of the cabinet at 40 000 × *g* for 45 min at 2 °C. The supernatant was made 2% (v/v) with buffer B (10 mM potassium

(17) Popescu, C. V.; Bates, D. M.; Beinert, H.; Munck, E.; Kiley, P. J. *Proc. Natl. Acad. Sci. U.S.A.* **1998**, *95*, 13431−13435.
(18) Jordan, P. A.; Thomson, A. J.; Ralph, E. T.; Guest, J. R.; Green, J. *FEBS Lett.* **1997**, *416*, 349−352.
(19) Lazazzera, B. A.; Beinert, H.; Khoroshilova, N.; Kennedy, M. C.; Kiley, P. J. *J. Biol. Chem.* **1996**, *271*, 2762−2768.
(20) Crack, J. C.; Green, J.; Le Brun, N. E.; Thomson, A. J. *J. Biol. Chem.* **2006**, *281*, 18909−18913.
(21) Sutton, V. R.; Mettert, E. L.; Beinert, H.; Kiley, P. J. *J. Bacteriol.* **2004**, *186*, 8018−8025.
(22) Crack, J. C.; Green, J.; Cheesman, M. R.; Le Brun, N. E.; Thomson, A. J. *Proc. Natl. Acad. Sci. U.S.A.* **2007**, *104*, 2092−2097.
(23) Miller, J. H. *Experiments in Molecular Genetics*; Cold Spring Harbor Laboratory Press: New York, 1972.
(24) Sutton, V. R.; Kiley, P. J. *Methods Enzymol.* **2003**, *370*, 300−312.

phosphate, 800 mM KCl, 10% (v/v) glycerol, pH 6.8) and loaded onto a 10 mL HiTrap SP FF cation-exchange column (GE Healthcare) previously equilibrated with buffer A. The column was washed with 15% (v/v) buffer B, and proteins were eluted using a linear gradient (60 mL) from 15% (v/v) to 100% (v/v) buffer B. Fractions containing FNR were pooled, diluted 3-fold with 10 mM potassium phosphate, 10% (v/v) glycerol, pH 6.8, and loaded onto a 2 mL HiTrap Heparin column (GE Healthcare) previously equilibrated with 5% (v/v) buffer B. The column was washed with 10% (v/v) buffer B and protein eluted using a linear gradient (50 mL) from 10% (v/v) to 100% (v/v) Buffer B. Fractions containing native FNR were pooled and concentrated as previously described.[24]

Purification of Reconstituted [4Fe−4S] FNR. Glutathione-*S*-transferase-FNR fusion protein was overproduced in aerobically grown *E. coli* BL21λDE3 pGS572 and purified as previously described using buffer C (25 mM 4-(2-hydroxyethyl)piperazine-1-thanesulfonate (Hepes), 2.5 mM $CaCl_2$, 100 mM NaCl, 100 mM $NaNO_3$, pH 7.5).[14] FNR was cleaved from the fusion protein using thrombin and [4Fe−4S] FNR reconstituted *in vitro*, as previously described.[14]

Quantitative Methods. FNR protein concentrations were determined using the method of Bradford[25] (BioRad), with bovine serum albumin as the standard, and a previously determined correction factor of 0.83.[14] FNR iron content was determined as previously described.[20] Acid-labile sulfide was determined according to the method of Beinert.[26] The concentration of dissolved atmospheric oxygen present in buffer solutions was determined by chemical analysis according to the method of Winkler.[27]

Spectroscopy. Absorbance measurements were made with a Jasco V550 UV−visible spectrophotometer. CD measurements were made with a Jasco J-810 spectropolarimeter. EPR measurements were made with an X-band Bruker ER300D spectrometer fitted with cavity type ER4116DM and an ESR-900 helium flow cryostat (Oxford Instruments). Spin intensities of paramagnetic samples were estimated by double integration of EPR spectra using 1 mM Cu(II), 10 mM EDTA as the standard.

Kinetic Measurements. Kinetic measurements were performed at 25 °C by combining varying aliquots of aerobic and anaerobic buffer (2 mL total volume) as previously described.[22] The reaction was initiated by the injection of an aliquot of native or reconstituted [4Fe−4S] FNR, and the mixture was stirred throughout. The dead time of mixing was ∼5 s. Changes in absorbance (at 420, 593, 562, or 523 nm) were used to track cluster conversion or formation of the $[Fe(II)(Ferene)_3]^{4-}$, $[Fe(II)(Ferrozine)_3]^{4-}$, and $[Fe(II)(2,2'\text{-bipyridyl})_3]^{2+}$ complexes, respectively. The structures of the iron chelators used in this study are given in Supporting Information Figure S1). Diffusion of dissolved atmospheric oxygen from the buffer into the head space of the sealed cuvette was assumed to be proportional to each initial starting oxygen concentration used in this study.[21] $[Fe(II)(Ferene)_3]^{4-}$ exhibited ϵ_{593nm} values of 32 243 M^{-1} cm^{-1} in buffer C and 39 600 M^{-1} cm^{-1} in buffer D (10 mM potassium phosphate, 400 mM KCl, 10% glycerol, pH 6.8) and buffer E (50 mM potassium phosphate, 400 mM KCl, 10% glycerol, pH 6.8).[20,21] $[Fe(II)(Ferrozine)_3]^{4-}$ and $[Fe(II)(2,2'\text{-bipyridyl})_3]^{2+}$ complexes exhibited ϵ_{562nm} and ϵ_{523nm} values of 24 163 M^{-1} cm^{-1} and 9101 M^{-1} cm^{-1}, respectively, in buffer C.

Data Analysis. The conversion of [4Fe−4S] FNR to [2Fe−2S] FNR was followed under pseudo-first-order conditions (with oxygen in excess) by measuring absorbance changes at 420, 523, 562, or 593 nm. Data sets were fitted to either a single exponential or where single-exponential fits were not satisfactory, to a double exponential function. Observed rate constants (k_{obs}) obtained from the fits (in the case of fitting to a double exponential function, the rate constant of the first reaction phase was used) were plotted against the corresponding initial concentration of oxygen to obtain the apparent second-order rate constant. Fitting of kinetic data was performed using Origin (Microcal).

Results

Optical and Magnetic Properties of Native and Reconstituted FNR. UV−visible absorbance spectra of anaerobic samples of native (isolated under anaerobic conditions) and reconstituted [4Fe−4S] FNR are shown in Figure 2A. Both spectra show absorption maxima at 320 nm ($\epsilon = 20\,075 \pm 350$ M^{-1} cm^{-1}) and 405 nm ($\epsilon = 16\,220 \pm 135$ M^{-1} cm^{-1}), together with a broad shoulder at 420 nm, consistent with previous reports.[14,20,21] Since the optical transitions of iron−sulfur clusters become optically active as a result of the fold of the protein in which they are bound, CD spectra reflect the cluster environment.[28] Anaerobic CD spectra of both native and reconstituted [4Fe−4S] FNR display three major positive features at 330, 380, and 420 nm; see Figure 2B.[14] The $\Delta\epsilon$ values for the native and reconstituted forms are very similar, indicating that the $[4Fe-4S]^{2+}$ clusters are in essentially identical environments. Moreover, they are of a similar magnitude to those of other proteins containing $[4Fe-4S]^{2+}$ clusters.[28,29]

Reaction of [4Fe−4S] FNR with oxygen leads to the formation of an $S = {}^1/_2$ $[3Fe-4S]^{1+}$ cluster intermediate.[14,22] To assess whether native and reconstituted $[4Fe-4S]^{2+}$ FNR generate similar EPR-active species, samples of both were exposed to a near stoichiometric amount of molecular oxygen and rapidly frozen for EPR analysis. Signals similar to that previously reported,[14,22] were observed in both samples, with indistinguishable properties; see Figure 2C. Spin integration of the signal by comparison with an integration standard revealed a maximum level of ∼15% of the original $[4Fe-4S]^{2+}$ cluster concentration, consistent with previous observations.[14,22]

Influence of Iron Chelators on the Rate of [4Fe−4S] to [3Fe−4S] FNR Cluster Conversion (Step 1). We recently showed that step 1 of the reaction of $[4Fe-4S]^{2+}$ FNR with oxygen is a second-order reaction with an apparent rate constant of $k_1 = 250 \pm 50$ M^{-1} s^{-1} at 25 °C.[22] These conclusions were based on kinetic measurements in which cluster conversion was followed directly, through the decay of absorption at 420 nm, and indirectly, through the complexation of Fe^{2+} released by the strong Fe^{2+} chelator Ferene, forming the highly colored complex $[Fe(II)(Ferene)_3]^{4-}$ (hereafter denoted as Fe^{2+}-Ferene). In the latter case, the experiments were performed in the presence of both Fe^{2+} and Fe^{3+} chelators since, in addition to Ferene, the experimental buffer contained 50 mM phosphate (buffer E).[22] Phosphate anions are well-known to form strong complexes with iron, with a preference for Fe^{3+}, with which it forms a highly insoluble complex.[30] Since similar results were observed for both direct and indirect measurements, it appears that the presence of iron chelators does not affect the oxygen-dependent conversion of [4Fe−4S] FNR to the intermediate [3Fe−4S] FNR species (step 1).

To probe this further, the effect of an Fe^{2+} chelator alone on step 1 was investigated by monitoring the formation of the Fe^{2+}-Ferene complex in a nonchelating buffer, 25 mM Hepes, pH 7.5 (buffer C). A_{593nm} as a function of time was measured for

(25) Bradford, M. M. *Anal. Biochem.* **1976**, *72*, 248−254.
(26) Beinert, H. *Anal. Biochem.* **1983**, *131*, 373−378.
(27) Vogel, A. I. *Vogel's Textbook of Quantitative Chemical Analysis*, 5th ed.; Longman Scientific and Technical: Harlow, U.K., 1989.
(28) Stephens, P. J.; Thomson, A. J.; Dunn, J. B.; Keiderling, T. A.; Rawlings, J.; Rao, K. K.; Hall, D. O. *Bochemistry* **1978**, *17*, 4770−4778.
(29) Stephens, P. J.; Jensen, G. M.; Devlin, F. J.; Morgan, T. V.; Stout, C. D.; Martin, A. E.; Burgess, B. K. *Biochemistry* **1991**, *30*, 3200−3209.
(30) Weast, R. C. *CRC Handbook of Chemistry and Physics*, 55th ed.; CRC Press: Boca Raton, FL, 1974.

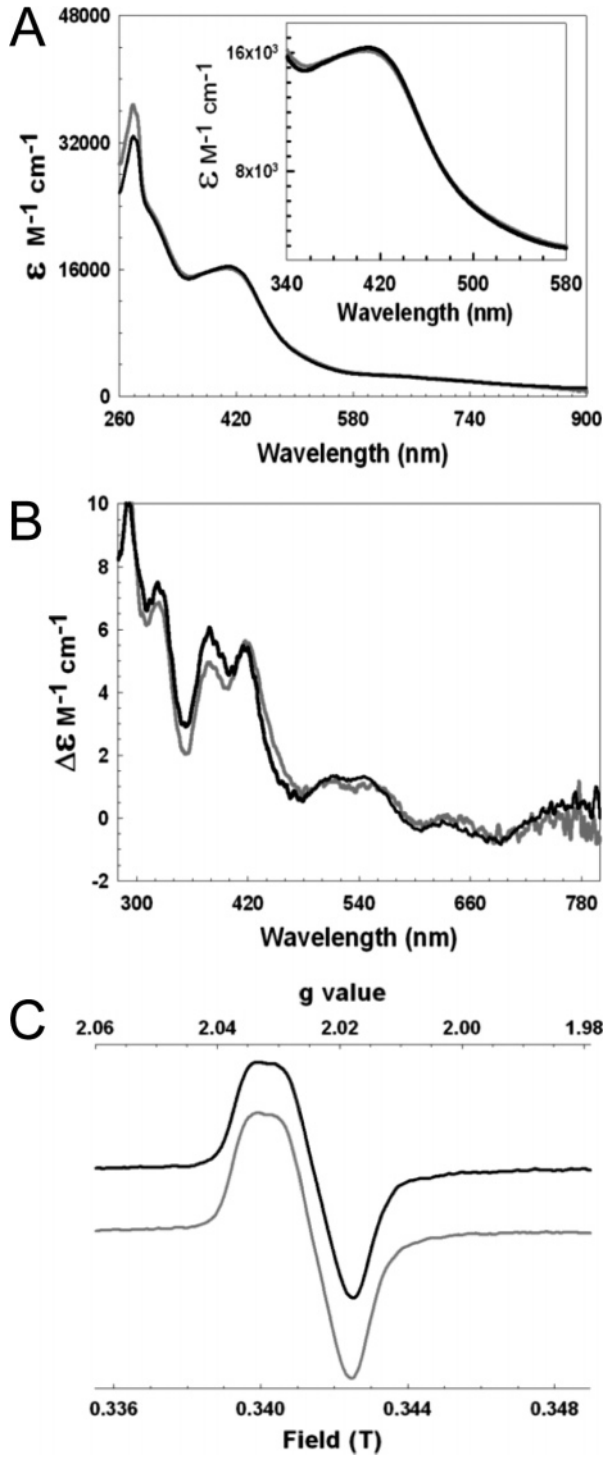

Figure 2. Spectroscopic comparison of native and reconstituted FNR: (A) Absorption spectra of native and reconstituted [4Fe−4S] FNR were recorded in 50 mM potassium phosphate pH 6.8 (Buffer E) and 25 mM Hepes pH 7.5 (Buffer C), respectively. (B) Comparison of the CD characteristics. CD spectra of native and reconstituted FNR were recorded in 10 mM potassium phosphate pH 6.8 (Buffer D) and 25 mM Hepes pH 7.5 (Buffer C), respectively. Extinction coefficients are relative to the $[4Fe-4S]^{2+}$ concentration. (C) An EPR comparison. [4Fe−4S] FNR was combined with an aliquot of aerobic buffer (∼150 μM [4Fe−4S], ∼185 μM O_2) and allowed to react (∼60 s) before being rapidly frozen in an EPR tube. The observed signals for native FNR (black) and reconstituted FNR (gray) corresponded to the conversion of ∼15% of the $[4Fe-4S]^{2+}$ cluster originally present. EPR spectra were recorded at 15 K, with a microwave power of 2.0 mW, a modulation amplitude of 0.5 mT, and a microwave frequency of 9.67 GHz. Spectra were normalized to the same receiver gain.

increasing oxygen additions to both native and reconstituted [4Fe−4S] FNR (2 μM) in the presence of Ferene (100 μM). Figure 3 shows data for reconstituted FNR. In contrast to experiments carried out in 50 mM phosphate, a single-exponential function did not provide good fits, although the data fitted well to a double exponential function. A plot of the observed pseudo-first-order rate constants for the first exponential phase, k_{obs}, against oxygen concentration was linear (Figure 3D), yielding an apparent second-order rate constant, k_1, at 25 °C of ∼300 M^{-1} s^{-1}, consistent with previous data.[22]

The effect of other strong Fe^{2+} chelators was also investigated. Equivalent experiments in the presence of either Ferrozine or 2,2′-bipyridyl (104 and 116 μM, respectively) were conducted in 25 mM Hepes pH 7.5 (buffer C). [4Fe−4S] FNR showed good stability in the presence of these chelators (although it was found to be somewhat less stable to these chelators than to Ferene), and neither was able to detect iron in solutions of Fe^{3+} in the absence of a reductant (data not shown). As in the case of Ferene, the Fe^{2+}-release was monitored through formation of the Fe^{2+}-chelator complex: $[Fe(II)(Ferrozine)_3]^{4-}$ (Fe^{2+}-Ferrozine) at 562 nm and $[Fe(II)(2,2'\text{-bipyridyl})_3]^{2+}$ (Fe^{2+}-bipyridyl) at 523 nm; see Figure 3B and C, respectively. Fitting of the data again required a double exponential function, and plots of the first observed rate constant for the Ferrozine and bipyridyl experiments as a function of oxygen concentration are shown in Figure 3D. The data for Ferrozine yielded an apparent second-order rate constant, k_1, of 300 M^{-1} s^{-1} at 25 °C, i.e., similar to that observed for Ferene, whereas the data for bipyridyl yielded $k_1 = 600$ M^{-1} s^{-1} at 25 °C. Thus, while Ferene and Ferrozine do not affect the rate of step 1, bipyridyl does, causing a doubling of the apparent second-order rate constant.

The effect of Fe^{3+} chelators on step 1 was also investigated in greater detail. We previously showed that measurements of 420 nm decay for both native and reconstituted [4Fe−4S] FNR in 50 mM phosphate revealed an essentially identical oxygen dependence as that observed for Ferene-mediated detection in the same buffer[22] and also in 25 mM Hepes (see above).

Equivalent experiments in which 420 nm absorbance decay was monitored were conducted in 25 mM Hepes (buffer C) with and without 600 μM ethylenediaminetetraacetate (EDTA), Figure 4A and B. In the absence of EDTA, a slow secondary reaction was observed to occur, and as a result, a double exponential function was required to fit the data. In the presence of EDTA, the slow reaction was less apparent and the data fitted well to a single-exponential function. Observed pseudo-first-order rate constants resulting from the first exponential (corresponding to the $[4Fe-4S]^{2+}$ to $[2Fe-2S]^{2+}$ cluster decay reaction) were plotted as a function of oxygen concentration; see Figure 3D. This revealed a similar oxygen dependence as observed for equivalent experiments in phosphate.[22] These data indicate that Fe^{3+} chelators do not significantly affect the rate of step 1.

Influence of Iron Chelators on the Rate of [3Fe−4S] to [2Fe−2S] FNR Cluster Conversion (Step 2). Step 2 of the conversion reaction was found, from 420 nm absorption and EPR $[3Fe-4S]^{1+}$ signal decay, to be an oxygen independent first-order reaction with an apparent rate constant of k_2 = ∼0.008 s^{-1}.[22] In our previous report, the Ferene assay in 50 mM phosphate buffer resulted in the detection of one Fe^{2+} ion

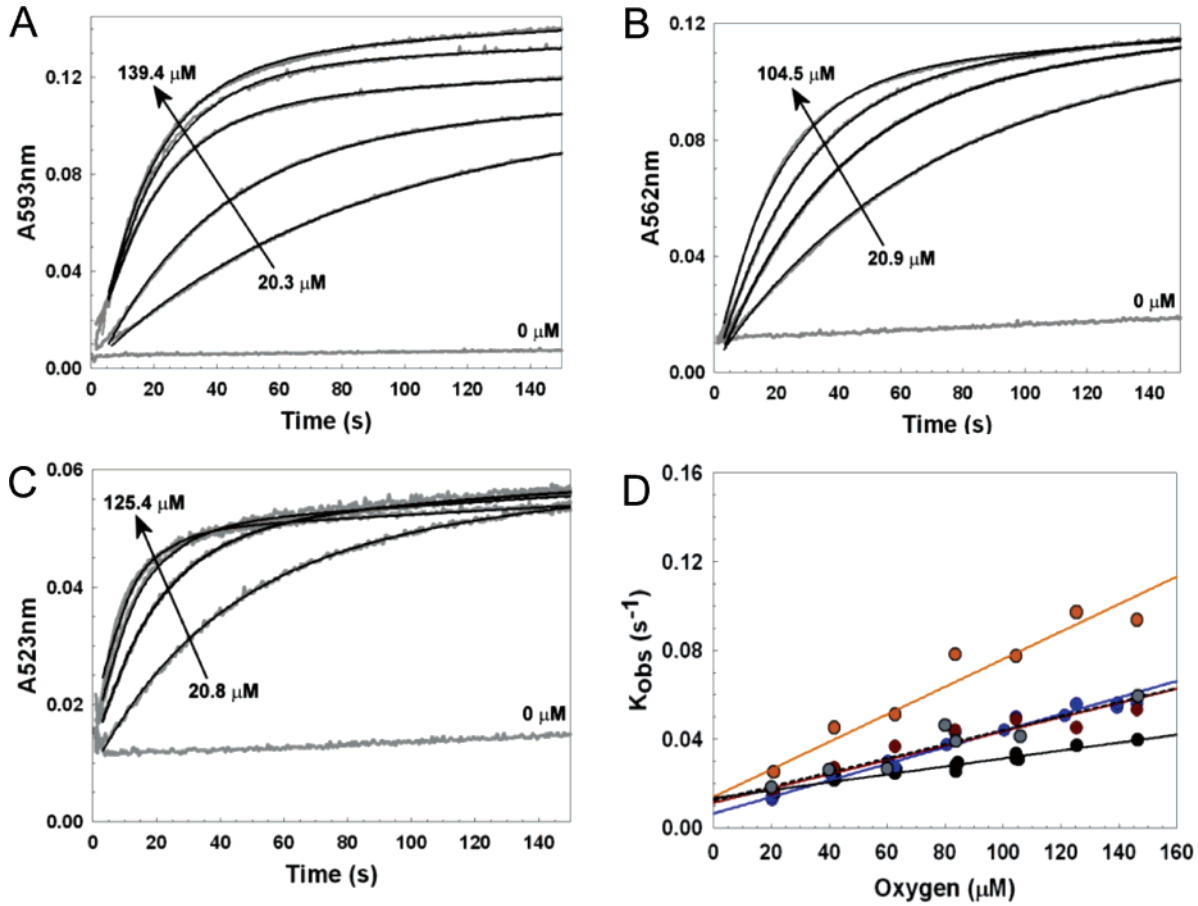

Figure 3. Effect of Fe^{2+}-chelators on the [4Fe−4S] FNR cluster conversion reaction: Plots of Fe^{2+} per [4Fe−4S] recovered by (A) Ferene, (B) Ferrozine, and (C) bipyridyl as a function of the oxygen concentration. Reconstituted [4Fe−4S] FNR (2 μM) was mixed with aliquots of buffer (25 mM Hepes pH 7.5 (buffer C)) containing varying concentrations of dissolved atmospheric oxygen at 25 °C. In each case, the reaction was initiated via injection of FNR. Release of Fe^{2+} from the [4Fe−4S] cluster was monitored with Ferene at 593 nm, Ferrozine at 562 nm, and bipyridyl at 523 nm. Double exponential function fits of the data are indicated by solid black lines. Arrows indicate the direction of response with increasing initial oxygen concentrations. (D) Plots of the first observed (first order) rate constants obtained from data in (A)−(C) from experiments conducted in Ferene (blue), Ferrozine (red), and bipyridyl (orange), and from the 420 nm decay data in Figure 4A (black) and B (gray), as a function of oxygen concentration. Least-squares linear fits of the data are shown, the gradient of which corresponds to the apparent second-order rate constant.

(resulting from step 1) and so did not provide any information on step 2.[22]

Figure 5 shows the total concentration of Fe^{2+} recovered via Fe^{2+}-chelator complexation (following oxygen induced cluster conversion) for the experiments described above. Where a double exponential function was required to fit the data, the amplitude of the first exponential phase was taken to indicate the amount of Fe^{2+} recovered in the initial phase; the iron released in the subsequent slow reaction was ignored for the purposes of the comparison because the slow reaction was not detected in phosphate buffer (see later for a further discussion of the slow reaction). In general, the Fe^{2+} detected under any one set of chelator conditions was found to be essentially independent of the oxygen concentration. Importantly, the amount of Fe^{2+} detected varied between ~1 and 2 per $[4Fe-4S]^{2+}$ cluster. Data for reactions in 50 mM phosphate (buffer E)[22] were also plotted to aid comparison. Data for Ferene in 25 mM Hepes (buffer C) was unusual in that it revealed an oxygen dependence: at low oxygen (~10 fold excess of oxygen over cluster) ~1 Fe^{2+} per cluster is detected, while at high oxygen (~60-fold excess) ~2 Fe^{2+} ions are detected per cluster.

The detection of >1 Fe^{2+} ion per cluster, at first sight, appears inconsistent with our mechanism for cluster conversion, in which one Fe^{2+} and one Fe^{3+} ion is ejected from the cluster. A consideration of the effect of chelators, however, resolves this apparent contradiction. The data indicate that Fe^{3+} released during cluster conversion is complexed by the Fe^{2+} chelators present and consequently becomes susceptible to reduction. In the presence of 50 mM phosphate, this secondary reaction is inhibited through the ability of phosphate to complex Fe^{3+}, which protects it from reduction, and, therefore, detection as Fe^{2+}. We previously demonstrated that the addition of a reductant to the phosphate reaction enabled the detection of 2 Fe^{2+} ions per cluster[22] and is, therefore, able to overcome the protective effect of phosphate.

To test this proposal further, cluster conversion reactions monitored by Fe^{2+}-Ferene complex formation were repeated in 25 mM Hepes (buffer C) in the presence of the Fe^{3+} chelator EDTA (670 μM). The presence of EDTA did not have a significant effect on the rate of step 1 (see Supporting Information Figure S2) consistent with 420 nm decay data (Figures 3D and 4B). Total Fe^{2+} recovered as a function of oxygen concentration is plotted in Figure 5: only 1 Fe^{2+} ion was recovered per cluster (independent of the oxygen concentration). Thus, EDTA can also protect Fe^{3+} against reduction.

Reactions in which both Fe^{2+} and Fe^{3+} chelators are present are of particular interest because there must be competition between the chelators for the available iron. To investigate this,

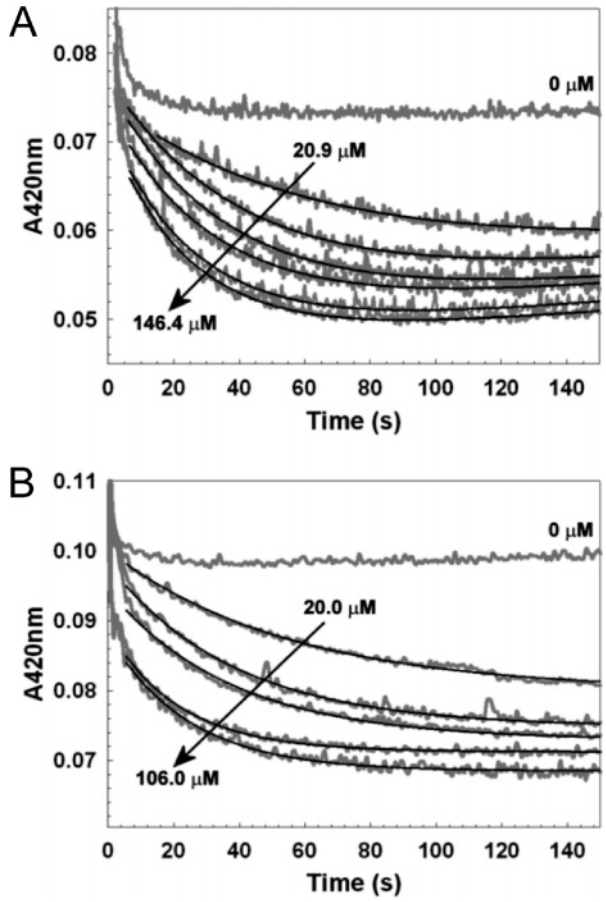

Figure 4. Effect of an Fe^{3+}-chelator on the [4Fe−4S] FNR cluster conversion reaction: (A and B) Reconstituted [4Fe−4S] FNR (5 μM) was mixed with aliquots of 25 mM Hepes pH 7.5 (buffer C) in the absence (A) and presence (B) of 670 μM EDTA containing varying concentrations of dissolved atmospheric oxygen at 25 °C. In each case, the reaction was initiated via injection of FNR. Loss of the [4Fe−4S] cluster was monitored at A_{420nm} as a function of time (in gray). Double exponential function fits of the data are indicated by solid black lines. Arrows indicate the direction of response with increasing initial oxygen concentrations.

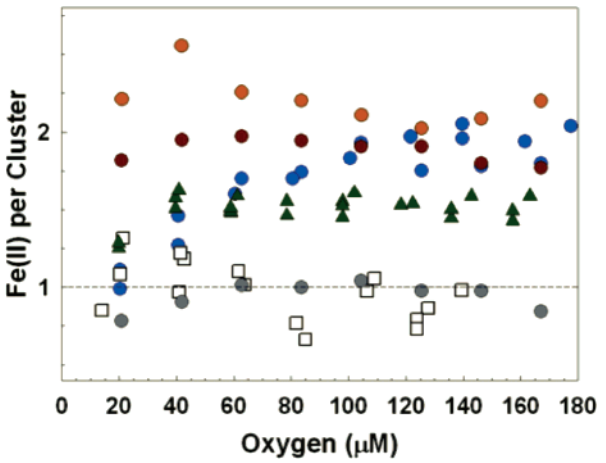

Figure 5. Environment dependence of Fe^{2+} recovered from [4Fe−4S] FNR upon oxidation: Plots of Fe^{2+} per [4Fe−4S] recovered by Fe^{2+} chelators under a range of different conditions as a function of the oxygen concentration. Measurements correspond to the same samples as those in Figure 3 (and Figures S2 and S3, Supporting Information). In the case of reactions in phosphate (buffers D and E), Fe^{2+}-Ferene was calculated once $A_{593\ nm}$ had reached a stable value, while, for reactions in 25 mM Hepes, the data were fitted to a double exponential function (see main text) and the amplitude of the first exponential was used to quantify the amount of complex present. [4Fe−4S] FNR in Hepes/Ferene (blue circles), Hepes/ferrozine (red circles), Hepes/bipyridyl (orange circles), Hepes/Ferene/EDTA (gray circles), 10 mM phosphate/Ferene (green triangles), or 50 mM phosphate/Ferene (open squares).

Ferene cluster conversion experiments were repeated at a lower concentration of phosphate buffer (10 mM, buffer D). As for the case of 50 mM phosphate (buffer E), a single exponential fitted the data well, and a plot of observed pseudo-first-order rate constants k_{obs} against oxygen concentration was consistent with the conclusion that Fe^{3+} chelators do not significantly affect the rate of step 1 (see Supporting Information, Figure S3). The total Fe^{2+} recovered as a function of oxygen, plotted in Figure 5, revealed that an intermediate value of 1.5 ± 0.1 Fe^{2+} ions per cluster was recovered. Thus, at a lower concentration of phosphate, the balance is shifted toward the Fe^{2+} chelator but not to such an extent that all ejected iron is detected as Fe^{2+}.

The detection of >1 Fe^{2+} per cluster during the initial rapid phase following the initiation of cluster conversion by oxygen is highly significant because it indicates that, under some experimental conditions, steps 1 and 2 have become kinetically indistinguishable. With the exception of reactions carried out in bipyridyl, the rate of step 1 was found to be essentially unaffected by the presence of chelators. This indicates that step 2 must be significantly enhanced in these reactions.

To investigate the relative rates of steps 1 and 2 further, the formation and decay of the $[3Fe-4S]^{1+}$ intermediate were investigated by EPR spectroscopy for reactions occurring under different chelator conditions. Experimental conditions (20 μM cluster, ~10-fold excess of oxygen) were the same as those previously reported in the absence of chelators.[22] Time-resolved EPR spectra recording for [4Fe−4S] FNR in the presence of 1 mM Ferene, Ferrozine, and bipyridyl are shown in Figure 6A−C. The $[3Fe-4S]^{1+}$ intermediate is observed under each set of conditions, but its kinetic profile is significantly altered compared with that in the absence of a Fe^{2+} chelator; see Figure 6D. There are insufficient data points to reliably fit the data to a two step reaction mechanism, but it is readily apparent that, for each Fe^{2+} chelator, the $[3Fe-4S]^{1+}$ intermediate signal decays more rapidly than in the wild-type case, demonstrating that the rate constant for step 2 has increased significantly such that it approaches that for step 1. For bipyridyl, only a small fraction (~10%) of the $[3Fe-4S]^{1+}$ intermediate is detected (even at 25 s), indicating that the decay of the intermediate occurs significantly faster than in the presence of both Ferene and Ferrozine. That the concentration of the intermediate does not undergo further significant decay suggests that a small proportion of the intermediate cluster is somehow stabilized in the presence of bipyridyl. Optical experiments (see above) demonstrated that bipyridyl enhanced step 1 (i.e., formation of the $[3Fe-4S]^{1+}$ intermediate). If step 2 was not also significantly enhanced we would have observed much higher concentrations of the $S = {}^1/_2$ intermediate species. Thus, the data are consistent with a significant enhancement of the rate of step 2.

Absorbance data from experiments in the presence of Ferene in 50 mM phosphate[22] or 25 mM Hepes/EDTA (Figure S2, Supporting Information) did not give any information on the kinetic properties of step 2 (because only Fe^{2+} released in step 1 was detected). However, data for experiments in 10 mM phosphate, which revealed the recovery of 1.5 Fe^{2+} per cluser in the initial (single exponential) phase, indicated that Fe^{3+} chelators must also affect the rate of step 2. Thus, similar EPR

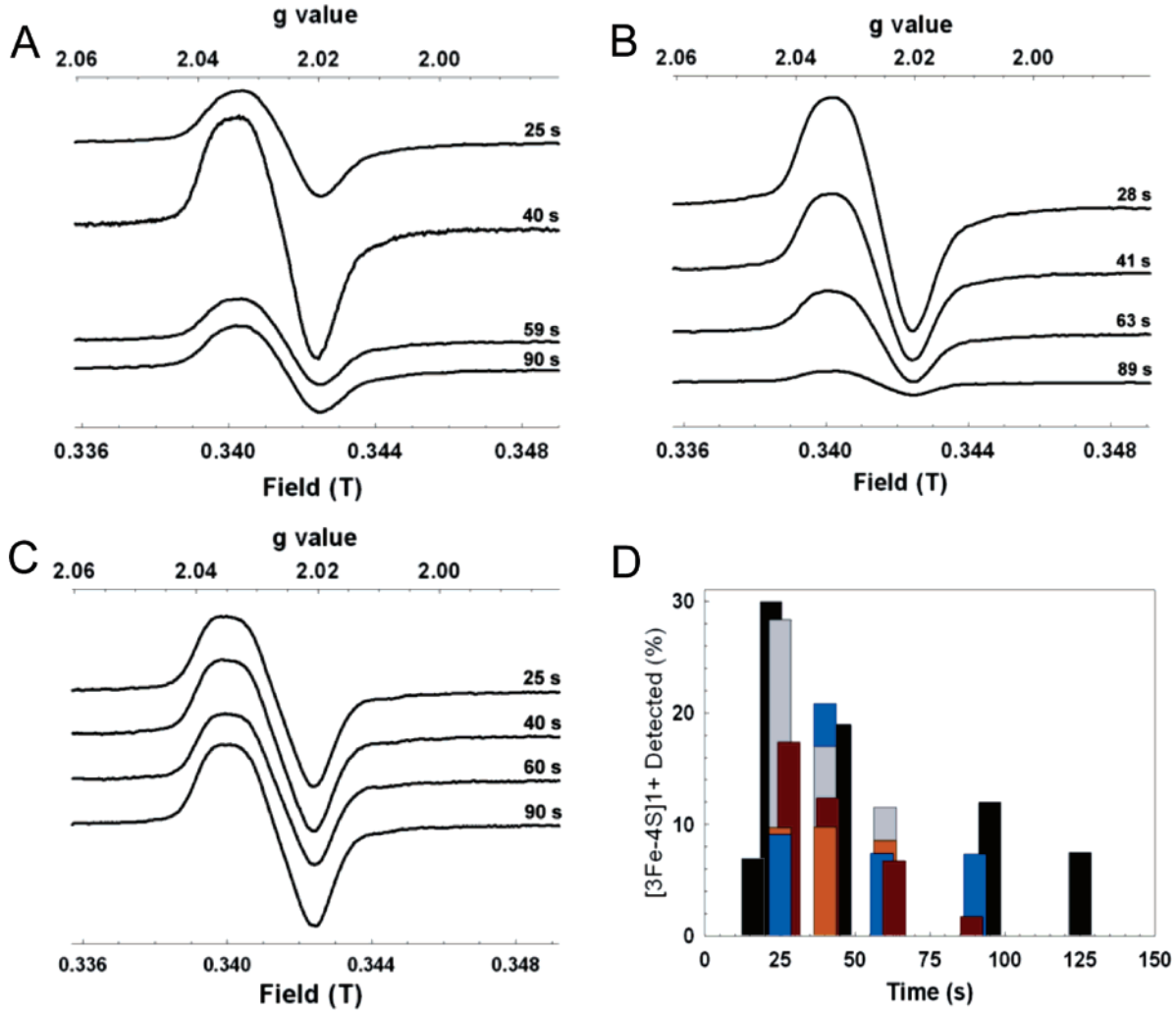

Figure 6. Effects of Fe^{2+} chelators on the detection of $[3Fe-4S]^{1+}$ intermediate cluster during the oxidation of [4Fe−4S] FNR: EPR spectra of reconstituted [4Fe−4S] FNR (20.2 μM) in 25 mM Hepes (Buffer C) and (A) Ferene (1 mM), (B) ferrozine (1 mM), and (C) bipyridyl (1 mM) at increasing time points following exposure to dissolved atmospheric oxygen (219.5 μM, 21 °C). EPR spectra were recorded using the same parameters as those in Figure 2C, and spectra were normalized to the same receiver gain. (D) Bar chart representation of $[3Fe-4S]^{1+}$ signal intensity observed under different chelator conditions (expressed as a percentage of the original $[4Fe-4S]^{2+}$ concentration) as a function of time. Hepes (black), Hepes/Ferene (blue), Hepes/Ferrozine (red), Hepes/bipyridyl (orange), Hepes/Ferene/EDTA (gray).

experiments were conducted for [4Fe−4S] FNR in 50 mM phosphate buffer (buffer E); see Figure 7A. Signal intensity due to the $[3Fe-4S]^{1+}$ intermediate is completely absent at 40 s, and measurements at other time points similarly completely lacked $[3Fe-4S]^{1+}$ intensity (not shown). We conclude that, in the presence of 50 mM phosphate, the rate of step 2 is enhanced to the extent that the intermediate species can no longer be detected. Time-resolved EPR experiments were conducted in the presence of 6 mM EDTA; see Figure 7B. The concentration of the $[3Fe-4S]^{1+}$ intermediate (expressed as a percentage of the original $[4Fe-4S]^{2+}$ concentration) is plotted as a function of time, Figure 6D. Again the data show an enhanced rate of decay of the intermediate species compared to that in the absence of chelators, indicating that the rate constant for step 2 is significantly enhanced. Single time point experiments (in which samples were frozen at ~40 s) conducted using FNR samples in 1 and 10 mM EDTA in 25 mM Hepes (buffer C) were also performed; see Figure 7A. At the lower concentration, EDTA has little effect on the appearance of the $[3Fe-4S]^{1+}$ intermediate (compared to the absence of chelators), while at a 10-fold increased concentration only a minor amount (~6%) of the $[3Fe-4S]^{1+}$ intermediate is observed. Thus, phosphate and EDTA exert a similar effect on step 2, although the chelator concentration dependence is different in each case.

Sulfide as a Possible Source of Electrons for Reduction of Fe^{3+} Released in Step 2 of Cluster Conversion. Here we have demonstrated that, in the presence of strong Fe^{2+} chelators, Fe^{3+} released in step 2 is susceptible to reduction. The kinetic characteristics of this reaction indicate that reduction must occur rapidly following release from the cluster (because step 1 and step 2 cannot be kinetically distinguished in these experiments). This implies that there is a readily available supply of electrons. To investigate whether sulfide is a possible source of electrons, reactions containing $FeCl_3$ (6.4 μM) and Ferene were incubated in the presence of excess glutathione (1.1 mM), or sulfide ions (20.8 μM, as Na_2S), or a mixture of the two (see Supporting Information Figure S4). When both sulfide and glutathione were present the Fe^{2+}-Ferene complex was formed at a significant rate under aerobic conditions (k_{obs} = ~0.002 s^{-1}; Supporting Information Figure S4). This indicates that sulfide ions are oxidized readily by Fe^{3+} ions in the presence of Ferene and suggests that sulfide could be one of the sources of electrons

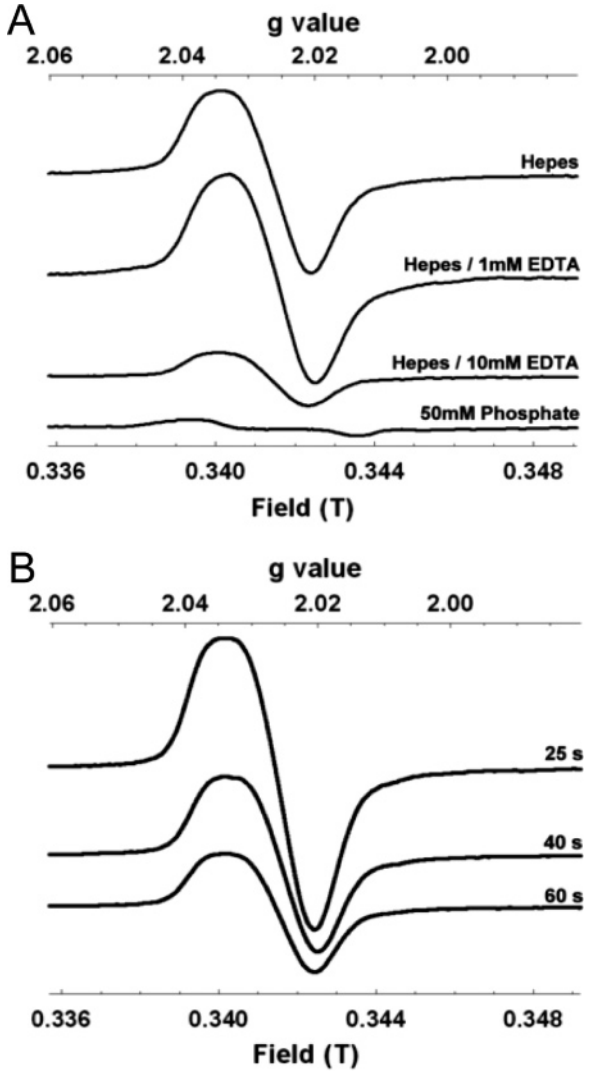

Figure 7. Effects of Fe^{3+} chelators on the detection of $[3Fe-4S]^{1+}$ intermediate cluster during the oxidation of [4Fe−4S] FNR: (A) EPR spectra of reconstituted [4Fe−4S] FNR (20.2 μM) in 50 mM phosphate (buffer E) or 25 mM Hepes (buffer C) in the absence of a Fe^{3+} chelator, and the presence of 1 mM and 10 mM EDTA, as indicated. Each spectrum was recorded for samples frozen 40 s after the introduction of oxygen. (B) EPR spectra of reconstituted [4Fe−4S] FNR (20.3 μM) in 25 mM Hepes, 6 mM EDTA at increasing time points following exposure to dissolved atmospheric oxygen (219.5 μM, 21 °C). EPR spectra were recorded using the same parameters as those in Figure 2C, and spectra were normalized to the same receiver gain.

for the reduction of Fe^{3+} released during step 2 of the reaction of the FNR [4Fe−4S] cluster with oxygen.

Discussion

Previous reports of mechanistic experiments probing the reaction of the FNR $[4Fe-4S]^{2+}$ cluster with oxygen, which leads to the formation of a single $[2Fe-2S]^{2+}$ cluster per monomer of the homodimeric regulator FNR, have used forms of FNR prepared in two different ways. One form, called native, is overexpressed in *E. coli* followed by anaerobic culturing and preparation. This yields a mixture of apo- and holoprotein containing variable amounts of the $[4Fe-4S]^{2+}$ cluster up to a maximum of ~70%. The other route, called reconstitution, uses an aerobic purification of apoprotein from *E. coli* followed by the NifS catalyzed insertion of a $[4Fe-4S]^{2+}$ cluster under reducing anaerobic conditions.[13,31] This enables a form of FNR to be obtained with typically ≥75% cluster occupancy.

In order to reconcile apparent inconsistencies in observations and resulting conclusions from different laboratories, it was suggested that the two differing routes of [4Fe−4S] FNR isolation might be important, such that reconstituted FNR reacts in a significantly different manner to native FNR following exposure to oxygen.[21] We have prepared FNR by both routes and subjected both forms to all the spectroscopic and kinetic experiments reported here, as well as those reported in our recent studies of sulfide release and cluster conversion.[20,22] We find no significant differences between the properties of these preparations of FNR. We therefore conclude that reconstituted and native proteins are identical, at least in their reactivity to oxygen *in vitro*.

Here we have investigated the oxygen-dependent conversion of the $[4Fe-4S]^{2+}$ cluster of FNR to the $[2Fe-2S]^{2+}$ form in more detail and, in particular, the effect that iron chelators have on the course of the reaction. The initial conversion of the $[4Fe-4S]^{2+}$ cluster to a $[3Fe-4S]^{1+}$ intermediate (step 1) is relatively insensitive to the presence of both Fe^{2+} and Fe^{3+} chelators. Only bipyridyl was found to have a significant effect, resulting in an increase of the apparent second-order rate constant from 250 to ~600 M^{-1} s^{-1} at 25 °C. Ferene and Ferrozine have similar structures and are both charged species at neutral pH, while bipyridyl is a neutral molecule. One possibility is that the greater hydrophobicity of bipyridyl enables it to approach the cluster and therefore exert an (albeit relatively small) influence of cluster reactivity.

The decay of the $[3Fe-4S]^{1+}$ intermediate to the $[2Fe-2S]^{2+}$ form (step 2) is much more readily influenced by iron chelators than step 1. Each of the Fe^{2+} chelators examined here was observed to enhance step 2, albeit to somewhat different extents. In the case of Ferrozine, ~2 Fe^{2+} ions were recovered in the initial phase following addition of oxygen indicating that steps 1 and step 2 are kinetically indistinguishable. EPR analysis of the appearance and decay of the $[3Fe-4S]^{1+}$ intermediate are consistent with this. A similar trend was observed for Ferene, although the effect on step 2 was less dramatic, consistent with the detection of ~1 Fe^{2+} under equivalent conditions of the cluster/oxygen ratio (i.e., 1:10) in UV−visible absorbance experiments. In the presence of bipyridyl, only a minor fraction of $[3Fe-4S]^{1+}$ was detected, consistent with the reaction occurring more rapidly than in the presence of Ferrozine or Ferene. The small proportion of cluster detected does not appear to decay away, suggesting that a small fraction of the $[3Fe-4S]^{1+}$ intermediate is stabilized by the chelator, again possibly reflecting the different electrostatic properties of this molecule.

The effect of Fe^{3+}-chelators on step 2 was also found to be very significant: in 50 mM phosphate, the $[3Fe-4S]^{1+}$ intermediate was not observed at all, indicating that step 2 is enhanced to the point that step 1 becomes the rate determining step of the cluster conversion reaction. Similar behavior was observed for another Fe^{3+} chelator, EDTA, and as might be expected, this was dependent on the concentration of the chelator. 1 mM EDTA (50-fold excess of chelator over cluster) did not have a significant effect on the appearance of the

(31) Zheng, L.; White, R. H.; Cash, V. L.; Jack, R. F.; Dean, D. R. *Proc. Natl. Acad. Sci. U.S.A.* **1993**, *90*, 2754−2758.

intermediate, whereas 10 mM EDTA (500-fold excess) had a very significant effect.

The much greater effect of iron chelators on step 2 of cluster conversion suggests that the $[3Fe-4S]^{1+}$ cluster is much more accessible to small molecules than the $[4Fe-4S]^{2+}$ form, consistent with the opening up of the cluster prior to the ligand rearrangement that accompanies the $[3Fe-4S]^{1+}$ to $[2Fe-2S]^{2+}$ conversion.

The data presented here demonstrate that Fe^{3+} released in step 2 is susceptible to reduction. In the absence of a competing Fe^{3+} chelator, $\sim$2 Fe^{2+} ions are recovered per cluster upon reaction with oxygen. The redox potential of the Fe^{3+}/Fe^{2+} couple is highly dependent on its environment. For example, the midpoint potential of the aqueous Fe^{3+}/Fe^{2+} couple shifts from +0.77 V to +0.96 V upon complexation with bipyridyl[32] and to −0.20 V upon complexation with EDTA.[32] Thus, the reduction of Fe^{3+} to Fe^{2+} is favored in the presence of an Fe^{2+} chelator and inhibited in the presence of an Fe^{3+} chelator (which would instead favor oxidation of Fe^{2+} to Fe^{3+}). Therefore, in the presence of both Fe^{2+} and Fe^{3+} chelators, a competition for the available iron exists, and the relative affinities for iron, concentrations, and solubilities (of iron complexes) become important in determining the final speciation of the iron. Fe^{2+} forms very tight complexes with the Fe^{2+} chelators employed here ($\log \beta_3 = 14.9 - 17.6$),[33−35] while EDTA forms an extremely tight complex with Fe^{3+} ($\log K = \sim 25$).[36] The chemistry of Fe^{3+} and phosphate is complex but is ultimately dominated by the extremely low solubility of ferric phosphate, which results in the removal of Fe^{3+} from solution. Here, we have found that, at 50 mM phosphate or 670 μM EDTA (and 106 μM Ferene), all of the released Fe^{3+} remains as Fe^{3+}, whereas at 10 mM phosphate (under the conditions tested here) there is a roughly equal partition between chelators. Note that Fe^{3+} chelators have not been observed to compete for the Fe^{2+} ion released in step 1, suggesting that this iron is somehow protected from oxidation.

The detection of ejected Fe^{3+} as Fe^{2+} requires a ready source of electrons. Control experiments demonstrated that, under aerobic conditions in the presence of Ferene, glutathione, and sulfide, Fe^{3+} ions can be rapidly reduced. The high affinity of Ferene for Fe^{2+} compared with Fe^{3+} ions shifts the Fe^{3+}/Fe^{2+} potential strongly positive making Fe^{3+} a powerful oxidizing agent under these conditions. Consequently, sulfide ions released from the cluster, together with thiol groups of cysteine residues present within apo-FNR, may act as reductants of Fe^{3+} in the presence of Ferene and other Fe^{2+}-chelators during the step 2 reaction. Similar chemistry is likely to occur during the reaction of [4Fe−4S] FNR with oxygen, which results in increasing concentrations of sulfide, Fe^{2+}, and Fe^{3+} ions. In summary, the oxidation states in which the iron ions ejected from the FNR cluster are *detected* is dependent upon the chelating and redox properties of the medium into which it is released.

The data presented here enable us to understand why different laboratories have arrived at quite different conclusions in respect of the mechanism of the cluster conversion reaction. Sutton and co-workers proposed a concerted single step mechanism based on experiments conducted in phosphate buffer/Ferene.[21] We have demonstrated here that, under such conditions, step 2 occurs at a significantly enhanced rate such that the reaction rate is determined by the rate of the step 1, oxygen dependent reaction, and the $[3Fe-4S]^{1+}$ intermediate becomes difficult to detect; thus, the reaction *appears* to occur in a single step.

[2Fe−2S] FNR is not a stable species and slowly decomposes to apo-FNR both *in vivo* and *in vitro*.[37] The data presented here appear to give information on the breakdown of the $[2Fe-2S]^{2+}$ cluster. Cluster conversion reactions carried out in the presence of Fe^{2+}-chelators resulted in the observation of a slow reaction subsequent to the $[4Fe-4S]^{2+}$ to $[2Fe-2S]^{2+}$ switch (from which two Fe^{2+} ions are recovered), which resulted in the detection of further iron (as Fe^{2+}). Plots of the second observed rate constant (from the double exponential function that was required to accurately fit the data) against the oxygen concentration revealed an oxygen independent slow reaction with $k_2 = 0.0023 \pm 0.0007\ s^{-1}$ (not shown). Quantitation of the Fe^{2+} detected during this slow phase revealed the recovery of a further $\sim$1 Fe^{2+} per cluster for Ferene and Ferrozine but $\sim$2 Fe^{2+} per cluster for bipyridyl. We conclude that this slow reaction results from the slow breakdown of the $[2Fe-2S]^{2+}$ cluster to form, presumably, apo-FNR. When these reactions were conducted in phosphate (50 or 10 mM), the secondary, slow reaction was not detected, while in EDTA (670 μM) significantly less Fe^{2+} was detected in the slow phase ($\sim$0.5 Fe^{2+} per cluster). The conversion of [2Fe−2S] FNR to apo-FNR results in the ejection of two Fe^{3+} ions (as well as two S^{2-} ions). Clearly, the presence of an Fe^{3+}-chelator inhibits the detection of iron as an Fe^{2+}-complex. A similar slow reaction was also observed via 420 nm absorption measurements in 25 mM hepes (buffer C) but was less marked in the presence of EDTA.

Concluding Remarks

A rather full picture is now emerging of the molecular mechanism of the reaction of the $[4Fe-4S]^{2+}$ cluster of FNR with oxygen that is unexpected, even counterintuitive; see Scheme 1. An understanding of the influence of chelators on the FNR reaction reported here point to the possible significance of reactions which take place in the cytoplasm of the bacterial cell. The *E. coli* cell contains a whole range of molecules and macromolecules, some of which have the capacity to chelate either Fe^{2+} or Fe^{3+}, and others to provide a redox buffered environment, such as glutathione. The first step of the FNR trigger is a one electron process in which the product of oxygen reduction is a superoxide ion, a potentially toxic product.[22] We have shown that FNR itself possesses dismutase activity and this, together with the action of the intracellular enzymes SOD and catalase, very likely leads to recycling of the superoxide ion to oxygen and water. This allows one oxygen molecule to undergo a four electron reduction to water and, in the process, to oxidize four FNR clusters. The biological advantage is a 4-fold increase in the sensitivity of FNR to the analyte, oxygen. The generation of a $[3Fe-4S]^{1+}$ cluster, and loss of one Fe^{2+} ion, results in a reduced capacity of the cluster to bind the protein: it can bind only three protein cysteine ligands compared with four bound by the [4Fe−4S] cluster. This decrease in

(32) Phillips, C. S. G.; Williams, R. J. P. *Inorganic chemistry Part II*; Oxford University Press: Oxford, 1966.
(33) Sillen, L. G.; Martell, F. M. *Stability constants of metal ion complexes*, 2nd ed.; The Chemical Society: London, 1964.
(34) Hennessy, D. J.; Reid, G. R.; Smith, F. E.; Thompson, S. L. *Can. J. Chem.* **1984**, *62*, 721−724.
(35) Gibbs, C. R. *Anal. Chem.* **1976**, *48*, 1197−1201.
(36) Hutcheson, R. M.; Engelmann, M. D.; Cheng, I. F. *Biometals* **2005**, *18*, 43−51.
(37) Achebach, S.; Selmer, T.; Unden, G. *FEBS J.* **2005**, *272*, 4260−4269.

Scheme 1. Schematic Reaction Scheme for FNR Cluster Conversion[a]

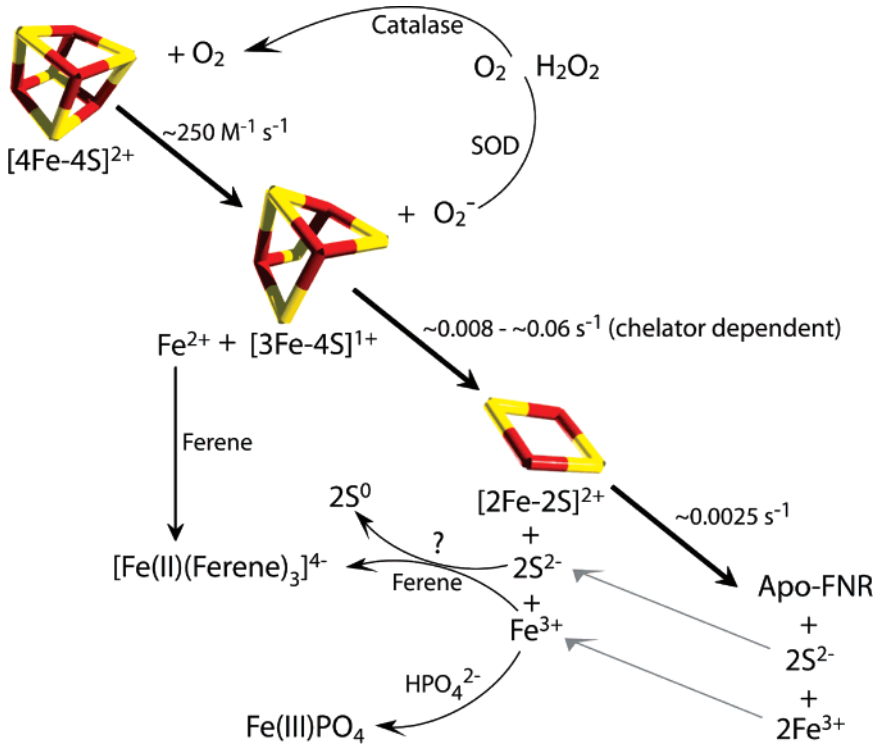

[a] The effect of Fe^{2+} and Fe^{3+} chelators is illustrated here by Ferene and phosphate, respectively.

protein cross-linking initiates a set of conformational changes and eventual monomerization that prevents FNR from binding its promoter target on DNA. The subsequent thermal degradation of the $[3Fe-4S]^{1+}$ cluster via a $[2Fe-2S]^{2+}$ cluster to apo-FNR ejects three Fe^{3+} and four sulfide ions. The release of intracellular Fe^{3+} is potentially toxic. Mechanisms to overcome this could be the sequestration of Fe^{3+} by intracellular polyphosphate. Phosphate is a major component of the cytoplasm environment, in which it fulfils several roles. Indeed, inorganic pyrophosphate/polyphosphate levels are modulated in response to the cellular environment and have been shown to be involved in the regulation of some types of stress response.[38] Alternatively, chelation of Fe^{3+} can, especially in a thiol environment, result in the rapid reduction to Fe^{2+} which can enter the iron transport and storage pathway. The sensitivity of FNR cluster conversion kinetics to chelators reported here reveals mechanisms by which the cell can fine-tune its response to the onset of aerobic conditions.

Acknowledgment. This work was supported by the Biotechnology and Biological Sciences Research Council Grant BB/C500360/1 and by a Wellcome Trust awards from the Joint Infra-structure Fund for equipment. We are grateful to Nick Cull for technical assistance, Professor Dennis Dean (Virginia Tech) for the plasmid pDB551, and to Belle Technology for their assistance with the anaerobic glove box fridge−freezer.

Supporting Information Available: Structures of Fe^{2+} and Fe^{3+} chelators used in this study (Figure S1); the effect of Ferene and EDTA on the [4Fe−4S] FNR cluster conversion reaction (Figure S2); the [4Fe−4S] FNR cluster conversion reaction in 10 mM phosphate (Figure S3); reduction of Fe^{3+} to Fe^{2+} in the presence of Ferene (Figure S4). This material is available free of charge via the Internet at http://pubs.acs.org.

JA077455+

(38) Shiba, T.; Tsutsumi, K.; Yano, H.; Ihara, Y.; Kameda, A.; Tanaka, K.; Takahashi, H.; Munekata, M.; Rao, N. N.; Kornberg, A. *Proc. Natl. Acad. Sci. U.S.A.* **1997**, *94*, 11210−11215.
(39) Guex, N.; Peitsch, M. C. *Electrophoresis* **1997**, *18*, 2714−2723.